Modulation of dADAR-dependent RNA editing by the *Drosophila* fragile X mental retardation protein

Balpreet Bhogal, James E. Jepson, Yiannis A. Savva, Anita S.-R. Pepper, Robert A. Reenan, and Thomas A. Jongens

Supplementary Information

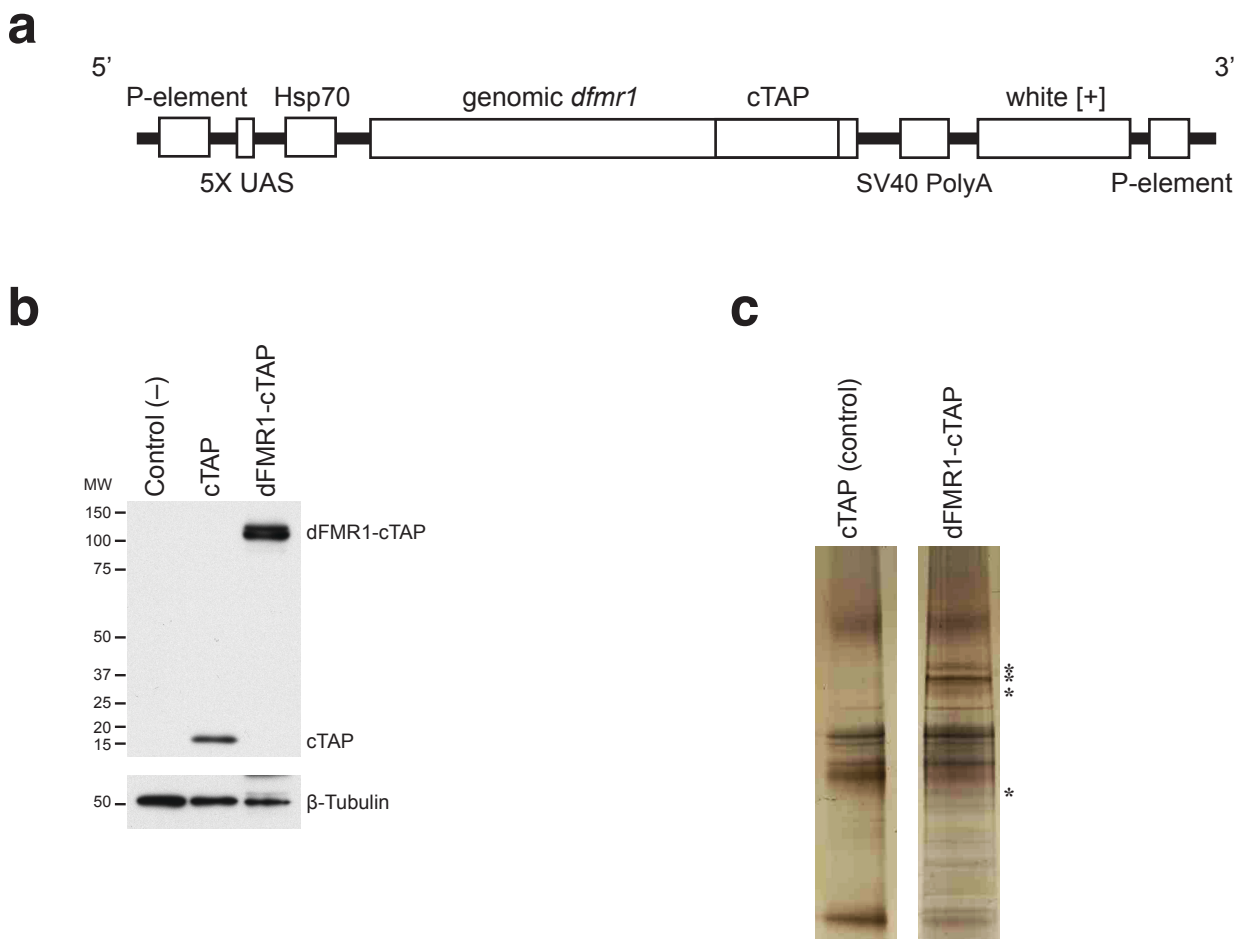

Supplemental Figure 1. TAP purification using S2 cells expressing a *pUAST-dFMR1-cTAP* construct. (**a**) Structure of the *pUAST-dFMR1-cTAP* construct used to generate stable S2 cell lines. The TAP tag sequence was inserted into the C-terminus (exon 12) of the genomic *dfmr1* rescue construct in the *pUAST* vector. Figure not drawn to scale. (**b**) Western analysis for dFMR1-cTAP or cTAP expression in S2 cells induced with $CuSO_4$ (final concentration 0.50 mM). Untransfected S2 cells were used as a negative control. An antibody against protein A was used to detect TAP-tagged constructs and anti-β-Tubulin was used as a loading control. Molecular weight (MW) is measured in kilodaltons (kDa). (**c**) The TAP protocol was carried out using protein extracts from S2 cells expressing dFMR1-cTAP or cTAP tag alone. Asterisks denote unique bands present only in dFMR1-cTAP pulldown lane that were excised for mass spectrometry analysis.

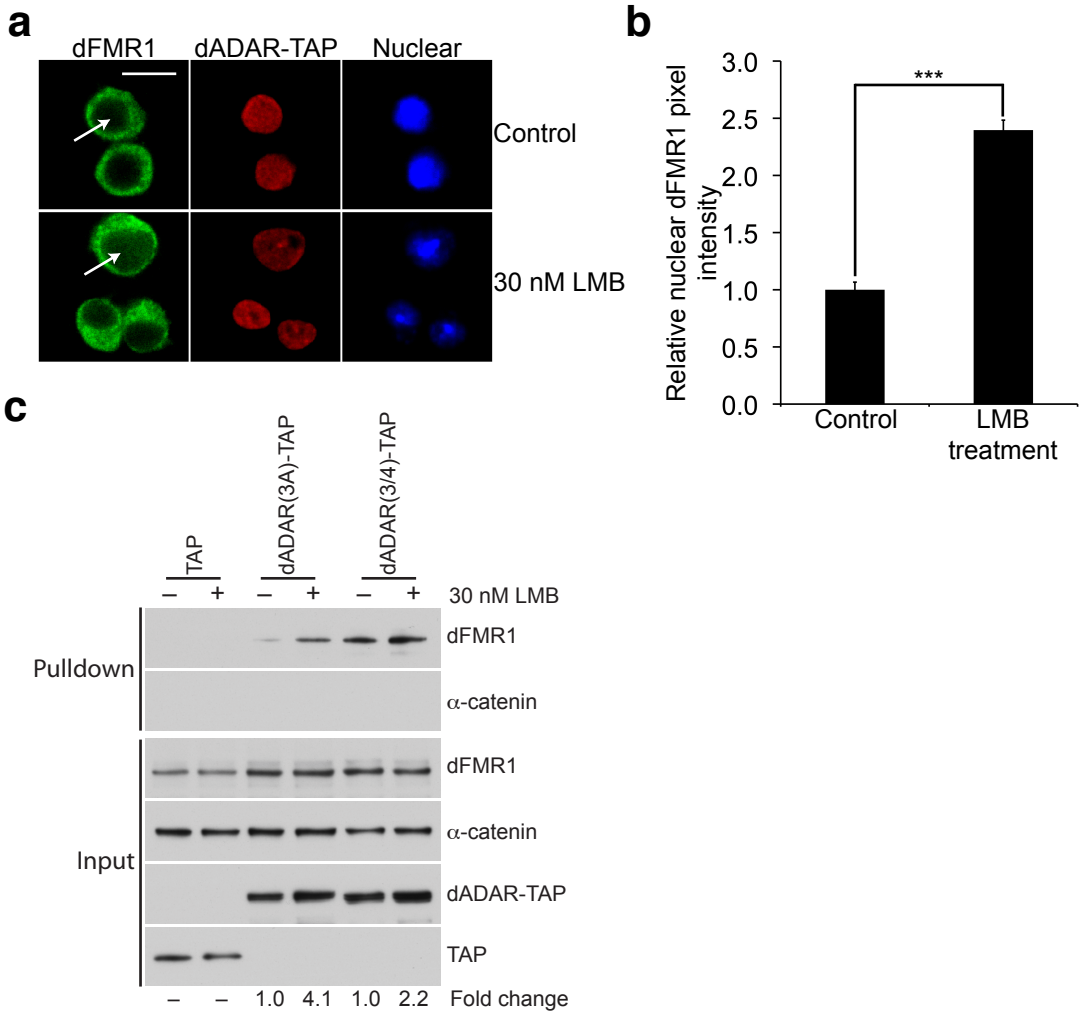

Supplemental Figure 2. Nuclear expression of dFMR1 and dADAR in S2 cells treated with leptomycin B. *Drosophila* S2 cells stably expressing dADAR(3/4)-TAP recombinant protein were treated with 30 nM leptomycin B (LMB) or methanol (vehicle control) to trap dFMR1 in the nucleus. (**a**) Representative confocal images of dADAR(3/4)-TAP-expressing S2 cells stained for dFMR1 (green), dADAR-TAP (red), and TO-PRO-3 (nuclear marker, blue) 4 hrs after LMB treatment. Arrows point to nuclear accumulation of dFMR1 in LMB-treated S2 cells (lower panels) compared to control-treated cells (upper panels). Scale bar represents 10 μm. (**b**) Quantification of nuclear dFMR1 in LMB-treated cells compared to control cells. Mean pixel intensity in dADAR(3/4)-TAP-expressing S2 cells treated with 30 nM LMB or vehicle control was quantified using ImageJ, and average pixel intensity in LMB-treated samples relative to control samples was plotted. n = 44 for control cells and n = 39 for LMB-treated cells. Error bars denote s.e.m. *** $p<0.0001$, analyzed by Student's *t*-test. Similar results were observed in S2 cells stably expressing dADAR(3A)-TAP (data not shown). (**c**) Tandem affinity purification on dADAR-TAP-expressing S2 cells treated with 30 nM LMB or vehicle control for 4 hrs. Samples treated with 30 nM LMB are designated as (+) and (–) samples denote vehicle control treatment. Relative dFMR1 expression in pulldown samples was normalized to dFMR1 expression in the input and average fold increase of the amount of dFMR1 pulled down with dADAR-TAP with LMB treatment relative to vehicle control cells for each cell line is denoted below lanes. α-catenin was used as a loading control and does not associate with dADAR-TAP. A FLAG antibody was used to detect TAP and dADAR-TAP constructs in input lanes. Experiments were performed three times.

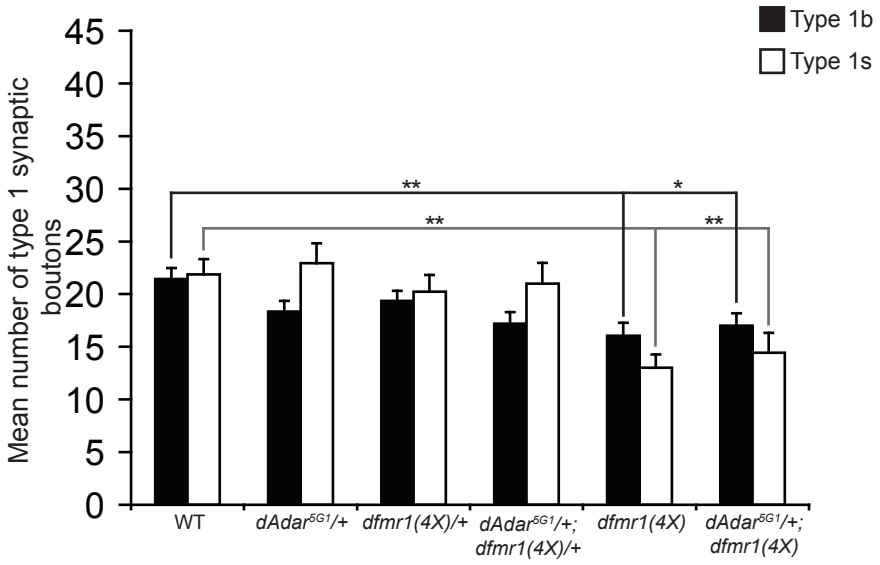

Supplemental Figure 3. Trans-heterozygous analysis using *dAdar^{5G1}* null and *dfmr1(4X)* overexpressing alleles. Reducing *dAdar* dosage in a *dfmr1(4X)* overexpressing fly background does not affect the *dfmr1(4X)* synaptic bouton phenotype. Quantification of average number of type 1b (black bars) and type 1s (white bars) synaptic boutons for trans-heterozygous genotypes using the *dAdar^{5G1}* null and transgenic *dfmr1(4X)* alleles. Flies containing the *dAdar^{5G1}* and/or *dfmr1(4X)* alleles were crossed to *w^{1118}* flies to collect larvae with one copy of each allele over wildtype. L3 larvae were stained with CSP and DLG. Type 1b and 1s boutons were distinguished as described in Fig. 2. Quantification was performed using muscles 6/7, hemisegment A3. n≥16. Error bars denote s.e.m. *p<0.05, **p<0.01, analyzed with one-way ANOVA, p<0.0001 overall, Tukey-Kramer post-test.

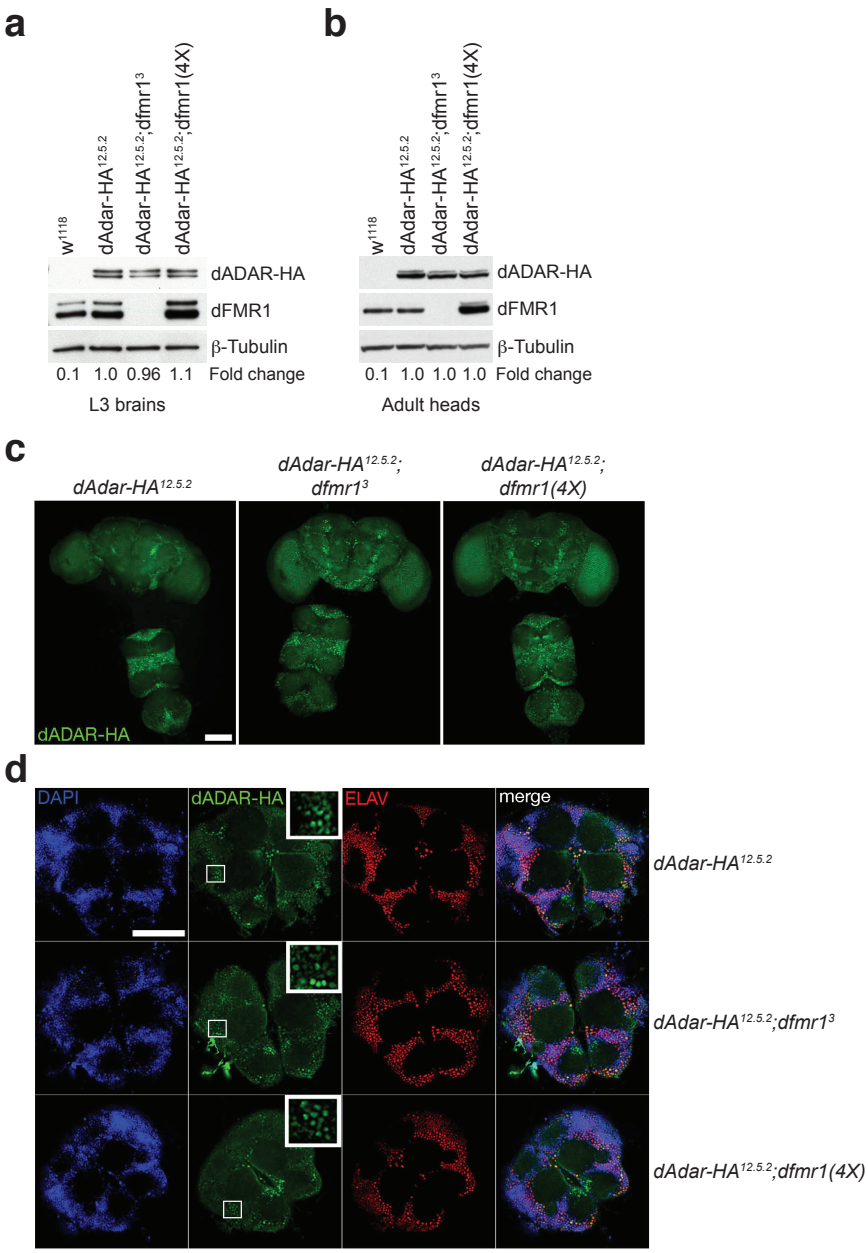

Supplemental Figure 4. dFMR1 does not affect dADAR expression levels or nuclear localization. The *dfmr1*^{3} null or *dfmr1(4X)* allele was crossed into the *dAdar-HA*$^{12.5.2}$ fly background to visualize dADAR expression through Western and immunohistochemistry analyses. (**a,b**) Lysates prepared from third instar larval brains (**a**) or adult fly heads (**b**) were run on SDS-PAGE electrophoresis followed by Western analysis. dADAR expression was visualized using an HA antibody (upper panels). An antibody against dFMR1 (middle panels) was used to show absence or overexpression of dFMR1 in the *dfmr1*^{3} or *dfmr1(4X)* backgrounds, respectively. β-Tubulin (lower panels) served as a loading control. *w*^{1118} flies served as a negative control for the HA antibody. Western analyses for both larval brain and adult head expression were run at least three times. dADAR-HA expression levels were normalized to β-Tubulin levels and average fold change of dADAR-HA expression relative to *dAdar-HA*$^{12.5.2}$ is denoted below lanes. (**c**) Immunostaining of dADAR-HA in adult male brains and thoracic ganglions in wildtype (*dAdar-HA*$^{12.5.2}$), *dfmr1*^{3} null (*dAdar*$^{12.5.2}$*;dfmr1*^{3}) and *dfmr1(4X)* overexpressing (*dAdar*$^{12.5.2}$*;dfmr1(4X)*) backgrounds. Scale bars represents 100 μm. (**d**) Loss or overexpression of dFMR1 does not alter dADAR-HA localization. Regardless of dFMR1 expression levels, dADAR-HA (green) co-localizes with both DAPI-stained DNA (blue) and ELAV (red), a marker for neuronal nuclei. Inset shows magnified image of nuclear dADAR localization. Scale bars represents 100 μm. Images are representative examples of n = 5.

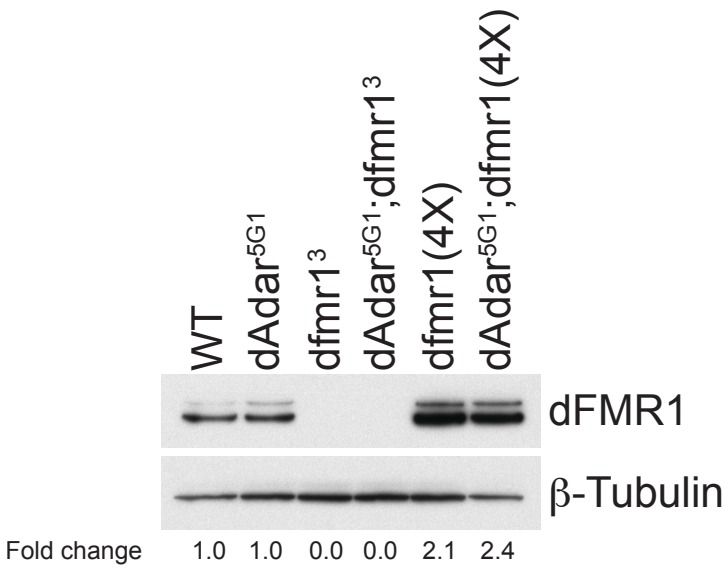

Supplemental Figure 5. Loss of dADAR expression does not affect dFMR1 levels. Western analysis on L3 larval brains from the following genotypes: *w*^{1118} (WT), *dAdar*^{5G1}, *dfmr1*^{3}, *dAdar*^{5G1}*;dfmr1*^{3}, *dfmr1(4X)*, and *dAdar*^{5G1}*;dfmr1(4X)*. An anti-dFMR1 antibody was used to detect dFMR1 levels (upper panel) and an antibody against β-Tubulin was used as a loading control (lower panel). Experiment was repeated three times. dFMR1 expression levels were normalized to β-Tubulin, and average fold change of dFMR1 expression relative to WT is denoted below lanes.

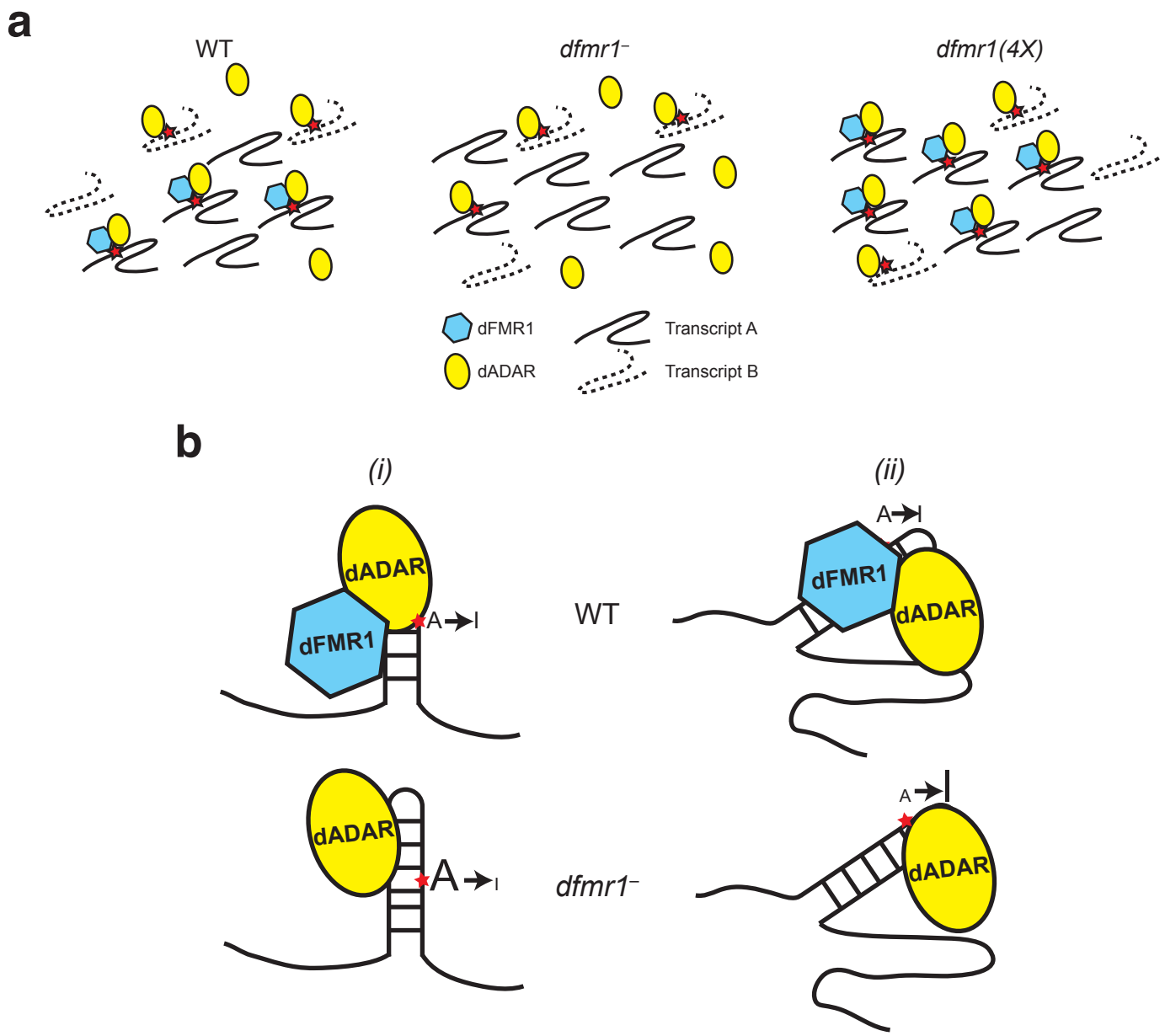

Supplemental Figure 6. Model: dFMR1 modulates dADAR activity in *Drosophila*. (**a**) We predict that dFMR1 and dADAR physically associate on transcripts that form secondary and more intricate RNA structures (transcript A). dADAR is also able to bind to highly structured RNA transcripts and edit independent of dFMR1 (transcript B). In the absence of dFMR1 expression, we predict that dADAR activity on the transcripts normally bound by both dFMR1 and dADAR is affected, and can consequently lead to a change in the normal editing activity. Although a reduction of editing is observed in (**a**), our results indicate that loss of dFMR1 can also lead to an increase in editing on certain sites and transcripts (see Fig. 7a). Red star denotes sites of active RNA editing. (**b**) Loss of dFMR1 expression results in differential effects on known edited sites, indicating that dFMR1 is affecting a subset of dADAR-dependent targets in specific manners. (i) In examples where the presence of dFMR1 enhances editing efficiency, dFMR1 may promote editing by recruiting dADAR to target sites (red star) or stabilizing higher order RNA structures targeted by dADAR, and when dFMR1 is absent, dADAR's association with its target site is weakened. (ii) In situations where dFMR1 negatively affects dADAR activity, dFMR1 may block an editing site targeted by dADAR or interfere with the formation of an dADAR substrate, which is alleviated when dFMR1 is absent.

Supplemental Table 1. Quantitative analysis of average number of type 1 synaptic boutons and branching in control genotypes of the Gal4/UAS rescue analysis. The number of hemisegments analyzed (n) and mean number of type 1 synaptic boutons and branching ± s.e.m. is given for each genotype. *βTub-Gal4* is a ubiquitous Gal4 driver, *elav-Gal4* and *scratch-Gal4* served as neuronal-specific Gal4 drivers, and *MHC-Gal4* and *G14-Gal4* were used for muscle-specific Gal4 drivers.

Supplemental Table 1. Genetic rescue of the *dAdar*^{5G1} null NMJ phenotype

Genotype	n	Bouton #	Branch #
w^{1118} (WT)	38	40.9 ± 1.2	3.6 ± 0.2
dAdar^{5G1}	24	64.6 ± 1.7*	6.2 ± 0.2*
dAdar^{5G1}*;UAS-dAdar/+*	16	67.8 ± 3.4*	6.0 ± 0.2*
dAdar^{5G1}*;UAS-dAdar/+;βTub-Gal4/+*	17	43.9 ± 2.0	3.9 ± 0.2
dAdar^{5G1}*;UAS-dAdar/+;elav-Gal4/+*	17	47.3 ± 2.3	4.0 ± 0.1
dAdar^{5G1}*;UAS-dAdar/+;scratch-Gal4/+*	16	39.6 ± 2.3	3.8 ± 0.3
dAdar^{5G1}*;UAS-dAdar/+;MHC-Gal4/+*	16	65.4 ± 3.0*	6.0 ± 0.3*
dAdar^{5G1}*;UAS-dAdar/G14-Gal4/+*	16	61.7 ± 2.1*	5.8 ± 0.3*
dAdar^{5G1}*;+;βTub-Gal4/+*	16	65.9 ± 3.1*	5.8 ± 0.3*
dAdar^{5G1}*;+;elav-Gal4/+*	21	60.1 ± 1.8*	5.7 ± 0.3*
dAdar^{5G1}*;+;scratch-Gal4/+*	16	62.8 ± 3.3*	6.1 ± 0.3*
dAdar^{5G1}*;+;MHC-Gal4/+*	19	67.3 ± 3.1*	5.9 ± 0.3*
dAdar^{5G1}*;G14-Gal4/+*	16	58.2 ± 2.3*	5.5 ± 0.3*
βTub-Gal4/+	18	44.7 ± 2.6	3.8 ± 0.3
elav-Gal4/+	22	44.2 ± 2.0	3.5 ± 0.3
scratch-Gal4/+	18	40.7 ± 1.8	3.5 ± 0.2
MHC-Gal4/+	17	40.5 ± 1.8	3.5 ± 0.2
G14-Gal4/+	16	42.1 ± 2.7	3.4 ± 0.2

Mean number of type 1 synaptic boutons and branching were scored using hemisegment A3, muscles 6/7.
Mean number of boutons/branches ± s.e.m. is listed for each genotype.
* $p < 0.001$ when compared to WT samples (one-way ANOVA, $p<0.0001$ overall, Tukey-Kramer post-test).